BMC Cardiovascular Disorders

RESEARCH

Open Access

Cardioprotective role of SIRT1 activation on mitochondrial function in insulin-resistant H9c2 cells

Buğrahan Sancak[1], Deniz İnönü[1], Gülsüm Alp[1], Faruk Tuna Sağlam[1], Leila Aryan[1,2,3], Suatnur Şık[1,4], Fırat Akat[5] and Erkan Tuncay[1,2,6*]

Abstract

Background Insulin-resistance in cardiomyocytes is often associated with metabolic disorders like obesity, and type2 diabetes. Studies demonstrated that sirtuin1 (SIRT1) plays a protective role in cells resistant to insulin by enhancing insulin sensitivity and improving glucose metabolism. Based on these protective functions observed in SIRT1, this study aims to investigate the roles of SIRT1 in palmitate (PA)-induced insulin-resistant H9C2 cells.

Methods Insulin-resistance was induced in H9c2 cells via incubation with palmitic acid (50μM;24 h). Control and Insulin-resistant cells were incubated with SIRT1 inhibitor (EX527;10μM) and SIRT1 activator (SRT1720;2μM) for 24 h, respectively. Mitochondrial membrane potential (MMP), reactive oxygen/nitrogen species (ROS/RNS), total ATP production, intracellular free zinc and calcium levels ($[Ca^{2+}]_i$ and $[Zn^{2+}]_i$) were monitored with fluorescence techniques. Protein levels were determined by using western-blot analysis.

Results K-acetylation level was increased in PA-induced Insulin-resistant cells and SIRT1 inhibited control cells. ROS/RNS production, $[Ca^{2+}]_i$, and $[Zn^{2+}]_i$ levels were elevated, MMP was depolarized and ATP production was decreased in PA and EX527 treated cells compared to control cells. Mfn1 and Fis1 levels were remained unchanged, however Mfn2 protein level was elevated in cells treated with PA and SIRT1 inhibitor. Nevertheless, anti- and pro-apoptotic protein level was reduced and augmented respectively in insulin-resistant and SIRT1 inhibited cells. Activation of SIRT1 in PA-treated cells restored mitochondrial function and intracellular ionic homeostasis, reduced K-acetylation, and mitigated apoptosis.

Conclusion Therefore, it can be proposed that the activation of SIRT1, acting as a novel regulator, may offer direct cardioprotection by restoring mitochondrial function in the insulin-resistant heart.

Keywords Cardiomyocytes, Insulin-resistant, SIRT1, Mitochondria, Calcium, Zinc

*Correspondence:
Erkan Tuncay
etuncay@medicine.ankara.edu.tr
[1]Department of Biophysics, Faculty of Medicine, Ankara University, Ankara, Türkiye
[2]Institute of Health Sciences, Ankara University, Ankara, Türkiye
[3]Stem Cell Institute, Ankara University, Ankara, Türkiye
[4]Department of Biochemistry, Faculty of Medicine, Hatay Mustafa Kemal University, Hatay, Türkiye
[5]Department of Physiology, Faculty of Medicine, Ankara University, Ankara, Türkiye
[6]Department of Neuroscience, Faculty of Medicine, Ankara University, Ankara, Türkiye

Introduction

Insulin resistance (IR) occurs when the insulin-sensitive tissues give lower glucose uptake responses to the same amount of insulin [1]. IR is one of the hallmarks of metabolic syndrome and Type II diabetes mellitus [2]. As far as IR is closely related to disrupted glucose homeostasis, it also causes various maladaptations at the cellular level. Palmitate-induced cellular insulin resistance model is widely used to mimic the systemic IR in cell culture [3].

Proteins in eukaryotic cells undergo diverse reversible post-translational modifications (PTMs), including glycosylation, phosphorylation, acetylation, and methylation that lead to dynamic alterations in their structure, stability, and function [4]. Dysregulation of PTMs has been implicated in various diseases and developmental disorders, emphasizing the critical role of PTMs in sustaining cellular equilibrium and functionality [5–8]. The acetylation process is the addition of an acetyl group to a peptide chain and serves as a critical regulator of numerous cellular pathways, controlling fundamental biological functions [4, 9, 10]. Acetylation of a lysine (K) residue in a peptide chain is called K-acetylation, which stands out as a key player among other acetylation types in the orchestration of function of proteins related to mitochondrial biogenesis, oxidative phosphorylation, and cellular energy metabolism [8, 11, 12]. Dysregulation of K-acetylation has been implicated in the pathogenesis of various cardiovascular diseases, including heart failure, hypertrophic cardiomyopathy, and myocardial ischemia, highlighting its potential as a therapeutic target for the development of innovative strategies aimed at preserving cardiac function and mitigating disease progression [8, 13]. The balance between acetyltransferase and deacetylase enzymes regulates the K-acetylation processes of various proteins [13–15].

Sirtuins (SIRTs) are a member of class-III histone deacetylase family that have Nicotinamide adenine dinucleotide (NAD^+)-dependent deacetylase ability and regulates the activity of numerous proteins in the cell [16, 17]. SIRT activity is one of the primary determiners of the K-acetylation level of the proteins inside the cell. For instance, K-Acetylation of cardiac sarcoplasmic reticulum calcium ATPase (SERCA2a) directly modulates the pumping function and disrupts intracellular calcium homeostasis in diabetic cardiomyopathy. Furthermore, application of resveratrol as a SIRT1 activator prevented this disruption by normalizing the SERCA2a function [18, 19]. SIRT 1 activity is reduced in insulin resistance and metabolic syndrome and this alteration is responsible for some of the metabolic disarrangements that we observe in these disease states. Furthermore, activation of the SIRT 1 cascade improves the tissue insulin sensitivity and protects the function and cell mass of pancreatic β-cells [20, 21].

Mitochondria are organized in a tubular, dynamic network that undergo continuous remodeling. These organelles can either divide *(fission)* or collide and fuse *(fusion)* in response to the needs of the cell [22]. Although a fused mitochondrial network is generally associated with higher and more efficient ATP yield and fission is associated with reduced respiration, mitochondrial fission is crucial for the removal of damaged mitochondria by mitophagy [23]. Therefore, mitochondrial energetics is orchestrated by a balance between fusion and fission [24, 25]. Mitochondrial fission is a more complex process compared to cellular division. Considering the two layered membrane structure of mitochondrion both inner and outer mitochondrial membranes have to be rearranged for fission in a coordinated manner. Mitofusins (MFNs) are outer membrane embedded proteins that have GTPase activity. Mitochondrial fission 1 protein (FIS1), MFN1 and MFN2 are considered to be main regulators of fission and fusion balance [26, 27].

The interaction between K-acetylation and intracellular free zinc levels $[Zn^{2+}]_i$ offer profound insights into the complex interplay of cellular signaling [28–30]. Furthermore, free zinc level is known to impact mitochondrial function, playing a pivotal role in the regulation of mitochondrial bioenergetics and redox homeostasis [31–33]. Disruptions in the crosstalk between K-acetylation, mitochondrial function, and zinc homeostasis have been implicated in various pathological conditions, including neurodegenerative disorders, metabolic diseases, and aging [13, 34].

Therefore, in the current study, we aimed to investigate the regulatory role of the K-acetylation process on cellular and mitochondrial functions in insulin-resistant H9c2 cells, and we hypothesized that intracellular free zinc level is a critical mediator between K-acetylation and mitochondrial bioenergetics. Understanding the intricate role of protein K-acetylation and zinc in the cardiomyocytes holds promise in unravelling the complex regulatory networks governing cardiac physiology and pathophysiology, thereby offering novel insights into the development of tailored therapeutic interventions for cardiovascular disorders.

Materials and methods

Cell culture and insulin-resistance model

The H9C2 line of embryonic rat ventricular cardiomyocytes (CRL-1446, ATCC; USA) were cultured at 37°C in Dulbecco's modified Eagle's medium (DMEM Low Glucose, Capricorn Cat No: DMEM-LPA Scientfic, Ebsdorfergrund, Germany) supplemented with %1 penicillin/streptomycin and heat-inactivated 10% fetal bovine serum, as previously described [8]. Palmitic acid (PA) (Sigma Aldrich, Cat No. P0500) incubation (50μM, 24 h) was used to induce insulin-resistance model in H9c2 cell

lines [35]. Insulin resistance was verified using a glucose uptake assay and by measuring the ratio of phosphorylated Akt protein to total Akt protein (Supplementary Fig. 1).

Western (immuno-) blot analysis

Cells were extracted with RIPA buffer containing EDTA and Protein Inhibitor Cocktail (Halt™ Protease and Phosphatase Inhibitor Cocktail, Cat No. 78440, Thermo Fisher; Massachusetts, USA). Homogenates were centrifuged at 10.000×g, 4 °C for 15 min. The supernatant was kept and total protein concentration was determined by the BCA assay kit (Pierce, USA; Cat no: 23225). Sample Buffer (4x Laemmli Sample Buffer, Cat. No:1610747, Biorad; California, USA) together with 5% β-mercaptoethanol as a reducing agent were added to homogenates. SDS-PAGE was executed with polyacrylamide gels as previously detailed [8]. An equal quantity of proteins was fractionated at 130 V for 15 min, followed by 110 V for 50 min before being transferred to polyvinylidene difluoride (PVDF) membranes. Blocking was accomplished by applying 5% BSA in TBS-Tween (0.05%) for 3 h, and the blots were left to incubate overnight at 4 °C with primary antibodies targeting the proteins: anti-Acetyl Lysine (Abcam ab21623; 1:2000), anti-Fis1 (Santa Cruz, sc-376447; 1:500), anti-Mfn1 (Santa Cruz, sc-166644, 1:1000), anti-Mfn2 (Santa Cruz, sc-100560, 1:1000), anti-Drp1 (Santa Cruz, sc-271583, 1:1000), anti-BAX (Santa Cruz, sc526; 1:1000), and anti-Bcl-2 (Santa Cruz, sc492; 1:1000), anti-Akt (Santa Cruz, sc-81434; 1:1000), and anti-pAkt (Santa Cruz, sc-101629; 1:1000). This was followed by a 1-hour incubation at room temperature with a blocking buffer containing secondary antibodies. Anti-β-actin (Santa Cruz, sc-47778, 1:5000) or anti-GAPDH (Cell Signalling, D16H11, 1:5000) were employed as housekeeping proteins to ensure even protein loading. Detection was achieved using chemiluminescence (SuperSignal™ West Dura Extended Duration Substrate, Thermo Scientific, USA; Cat no: 34075. Band intensities were evaluated using NIH image software (ImageJ), and the findings were presented as fold changes.

Measurement of mitochondrial membrane potential (ΔΨM)

Mitochondrial membrane potential (MMP or $\Delta\Psi_M$) in H9c2 cells was measured using a lipophilic, cationic fluorescence dye JC-1 (Invitrogen, T3168), as described previously [36, 37]. Briefly, cells were loaded with JC-1 dye (5μmol/L, 30 min) and imaged with a confocal fluorescence microscope (Leica TCS SP5, Germany). The probes were excited at 488 nm and the fluorescence image was detected at both 535 ± 15 nm (green; monomer form) and 585 ± 15 nm (red; J-aggregates form). Carbonylcyanide 4-(trifuoromethoxy) phenylhydrazone, FCCP (5μM acute application) was used for calibration. The fluorescence changes for MMP measurements were calculated according to the following formula: $F_{535/585}=F^0_{535/585}/F^1_{535/585}$ and F^0 represents the basal fluorescence level, while F^1 is the maximum fluorescence intensity after exposure to FCCP calculated from confocal images.

Measurement of reactive oxygen species (ROS) and reactive nitrogen species (RNS)

The total cellular ROS and RNS production were measured in H9c2 cells as described previously [38]. Briefly, cells were loaded with a ROS indicator chloromethyl-2′,7′-dichlorodihydrofuorescein diacetate, (DCFDA; 5μM for 1 h incubation), or RNS indicator Diacetate 4-Amino-5-Methylamino-2',7'-Difluorofluorescein Diacetate (DAF; 10μM for 1 h incubation), at room temperature. DCDFA or DAF was excited at 488 nm and the emission was collected at 560 ± 15 nm wavelengths with a laser scanning confocal microscope (LEICA TCS SP5, Germany). To obtain maximal fluorescence intensity associated with ROS or RNS production, the cells were perfused with hydrogen peroxide (H_2O_2; 100μM), or the nitric oxide (NO) donor sodium nitroprusside, (SNP; 100μM), respectively. The fluorescence changes, as peak values, ($\Delta F/F_0$, where $\Delta F = F - F_0$ and F_0 represents the basal fluorescence level, while F is the maximum fluorescence intensity after exposure to H_2O_2 or SNP is calculated from confocal images. All fluorescence changes to H_2O_2 or SNP are given as fold change changes in the manuscript.

Determination of intracellular free zinc ([Zn^{2+}]i)

Intracellular level of free Zn^{2+} ($[Zn^{2+}]_i$) in H9c2 cells was determined with a membrane permeable Zn^{2+-}sensitive fluorescence probe, FluoZin-3AM (Molecular Probes, Eugene, OR), as described previously [39]. Briefly, cells were loaded with FluoZin-3AM (3μM for 45 min) at room temperature. Probes were excited at 490 nm, and emission was collected at 525 ± 15 nm with a confocal microscope. $[Zn^{2+}]_i$ were determined using the following formula: $[Zn^{2+}]_i = Kd\ (F - F_{min})/(F_{max} - F)$, where the Kd is 15 nM. The maximum fluorescence intensity (F_{max}) was measured upon Zn^{2+} saturation with a zinc ionophore, Zn^{2+}-salt of 1-hydroxypyridine-2-thione, and Zn^{2+}-pyrithione (ZnPT; 10 μM), and the minimum fluorescence intensity (F_{min}) was measured upon an intracellular Zn^{2+} chelation with N, N, N′, N′-tetrakis (2-pyridylmethyl) ethylenediamine (TPEN; 50 μM).

Determination of intracellular free calcium ([Ca^{2+}]i)

The basal level of intracellular free Ca^{2+} ($[Ca^{2+}]_i$,) was measured in H9c2 cells loaded with calcium ion-specific ratiometric fluorescence dye Fura-2AM (4μM; 40 min) at room temperature, as described previously [40]. Briefly,

Fura-2 AM loaded cells were excited at 340 and 380 nm, and emissions were collected at 525 ± 15 nm, using the microspectrofluorometer (PTI Ratiomaster and FELIX software; Photon Technology International, Inc.). Emissions collected from F340/380 were used as an indicator of estimated $[Ca^{2+}]$i level.

Measurements of ATP level

The cellular level of ATP in H9c2 cell line was measured using a Luminescent based ATP assay kit (Promega, G9241), as described previously [41]. Equal amount of H9c2 cells were added to 96 well plates together with CellTiter-Glo 2.0 Reagent and incubated at room temperature for 10 min. Luminescence signals were recorded using a microplate reader.

Data analysis and statistics

All data were analysed and processed with a GraphPad Prism software 8.1 (GraphPad, San Diego, CA, USA). Data are presented as mean ± standard error of the mean (SEM). Comparisons between quantitative variables were determined by using unpaired two-sided Student's t-test or one-way ANOVA Tukey's multiple comparison tests were used for comparison between groups. *P* values < 0.05 were defined as statistically significant.

Chemicals

EX527 (Sigma-Aldrich Cat No. E7034) was used as a SIRT1 inhibitor (10 μM, 24 h), SRT1720 (Sigma-Aldrich Cat No. 567860) was used as a SIRT1 activator (2 μM, 24 h).

Results

Insulin resistance in cells refers to a condition where cells in the body, particularly in muscle, become less responsive to the effects of insulin [35, 41]. First, we confirmed that palmitic acid (PA)-induced insulin resistance in H9c2 cells by measuring glucose uptake and p-Akt protein levels. We found that glucose uptake and phosphorylated (p)-Akt levels in PA-induced insulin-resistant cells were significantly reduced compared to control cells, with only a limited decrease in total (T)-Akt levels. (Supplementary Figs. 1 and 6).

Hyper lysine (K)-acetylation of proteins can lead to detrimental consequences, including aberrant chromatin remodeling, dysregulated gene expression, and disrupted cellular signaling pathways, ultimately contributing to the pathogenesis of various diseases such as cancer, neurodegenerative disorders, metabolic dysregulation, and cardiovascular diseases [8, 42–44]. This increased K-acetylation can also impair protein-protein interactions, disturb cellular homeostasis, and disrupt critical biological processes, leading to cellular dysfunction and compromised physiological responses [34, 42]. Sirtuin1 (SIRT1) plays a pivotal role in regulating the K-acetylation status of proteins, modulating various cellular processes through its deacetylase activity and thereby impacting cellular physiology and disease pathogenesis [45]. We have tested whether SIRT1 inhibition or PA-induced insulin resistance alter the K-acetylation. Incubation of the H9c2 cells with SIRT1 inhibitor EX527 was significantly increased the total K-acetylation as well as in PA induced insulin-resistant cells. To understand the protective role of SIRT1 on K-acetylation, PA induced insulin-resistant cells were incubated with SIRT1 activator SRT1720. SIRT1 activation significantly reduced the total K-acetylation in insulin-resistant H9c2 cells (Fig. 1).

Maintaining intracellular ionic balance is vital for proper cardiac function, with increased levels of intracellular free Ca^{2+} $[Ca^{2+}]_i$ linked to contractile dysfunction. Dysregulation of $[Ca^{2+}]_i$ is associated with various conditions like diabetes, aging, and metabolic syndrome affecting the heart. $[Zn^{2+}]_i$ is also critical for cardiac function, as evidenced by our previous findings demonstrating that reduced $[Zn^{2+}]_i$ levels lead to decreased calcium transients, reduced SR calcium content, and diminished contractility in cardiomyocytes [46–48]. In this study, we investigated the impact of SIRT1 and insulin resistance on intracellular calcium ($[Ca^{2+}]_i$) and zinc ($[Zn^{2+}]_i$) levels in H9c2 cells. We observed that inhibiting SIRT1 or inducing insulin resistance with PA led to elevated $[Ca^{2+}]_i$ and $[Zn^{2+}]_i$ in cardiomyocytes (Fig. 2A-C). Conversely, activating SIRT1 in insulin-resistant cells markedly decreased both $[Ca^{2+}]_i$ and $[Zn^{2+}]_i$ levels (Fig. 2A-C).

Reactive oxygen species (ROS) and reactive nitrogen species (RNS) have a role on both physiological and pathophysiological processes in heart. It has been shown that excessive ROS and RNS production disrupts the ion channel function, changes the intracellular ionic homeostasis and decreases the cardiac contractility [47, 48]. Here, we observed that SIRT1-induced increased K-acetylation increased the ROS and RNS production as its observed in PA-induced insulin-resistant H9c2 cells. However, SIRT1 activation significantly prevented the increase in ROS and RNS production in insulin-resistant cells, either partially or completely (Fig. 3A-D).

Mitochondrial function is determined by various factors, including the membrane potential across the inner mitochondrial membrane, the regulation of mitochondrial fusion and fission processes, the levels of ROS and antioxidants, the energy demand, and mitochondrial biogenesis [37, 49]. Changes of these parameters determine the cell fate. Our findings demonstrated that insulin-resistant cells and SIRT1 inhibition notably caused mitochondrial membrane potential (MMP) depolarization, while SIRT1 activation significantly restored it in insulin-resistant cells (Fig. 4A and B). Additionally, we assessed ATP levels to investigate the impact of SIRT1-induced

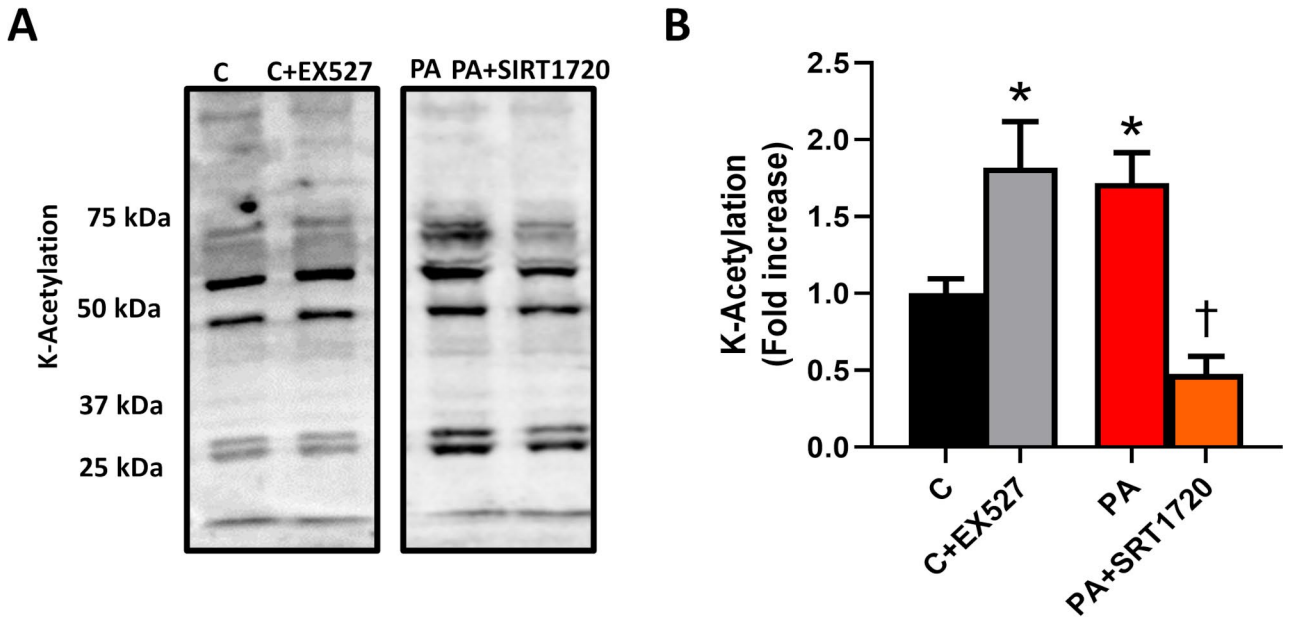

Fig. 1 SIRT1 inhibition and palmitic acid (PA)-induced insulin-resistant H9c2 cells exhibited elevated lysine (K)-acetylation. (**A**) The representative original Western Blot image to determine the total K-acetylation level in control (**C**) cells incubated with and without SIRT1 inhibitor (EX527;10μM), PA-treated insulin-resistant cells incubated with and without SIRT1 activator (SRT1720;2μM) for 24 h. (**B**) The mean values of total K-acetylation protein levels are given as bar graphs after divided by total protein levels (Supplementary File). EX527 was used as an inhibitor, and SRT1720 as an activator of SIRT1. Bars are represented as mean (± SEM). $N = 7–10$. Significance level accepted at $^{*}p < 0.05$ vs. C, and $^{\dagger}p < 0.05$ vs. PA

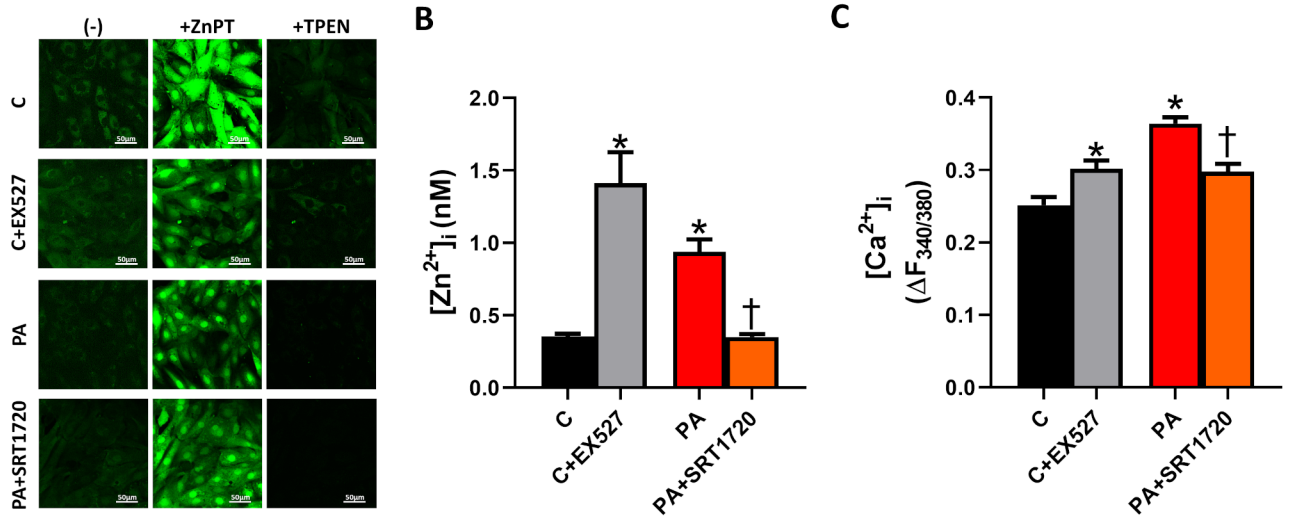

Fig. 2 The impact of SIRT1 inhibition and palmitic acid (PA)-induced insulin resistance on the levels of intracellular free zinc (($[Zn^{2+}]_i$) and calcium ($[Ca^{2+}]_i$). (**A**) Representative confocal images to determine the level of intracellular free Zn^{2+} ($[Zn^{2+}]_i$). (**B**) The bar graph shows the calculated $[Zn^{2+}]_i$ for the groups. The $[Zn^{2+}]_i$ was measured with a Zn^{2+}-selective fluorescence dye FluoZin-3AM. To determine the maximum and minimum fluorescence signals, the cells were treated with a zinc ionophore, Zn2+-pyrithione (+ ZnPT, 10μM), and a zinc-chelator, N,N, N′,N′-tetrakis(2-pyridinylmethyl)-1,2-ethanediamine (TPEN; 50μM), respectively. N_{cells}=50–80. (**C**) The bar graph represents the calculated intracellular free Ca^{2+} ($[Ca^{2+}]_i$) for the groups. The $[Ca^{2+}]_i$ was measured with a ratiometric Ca^{2+}-selective fluorescence dye Fura2-AM. Cells were excited at 340 and 380 nm, and emissions were collected at 525 ± 15 nm. Emissions derived from $F_{340/380}$ were utilized as an estimate of the $[Ca^{2+}]$i level. EX527 was used as an inhibitor, and SRT1720 as an activator of SIRT1. Bars are represented as mean (± SEM). The total number of cells used per group; n_{cells}=10–12. Significance level accepted at $^{*}p < 0.05$ vs. C, and $^{\dagger}p < 0.05$ vs. PA

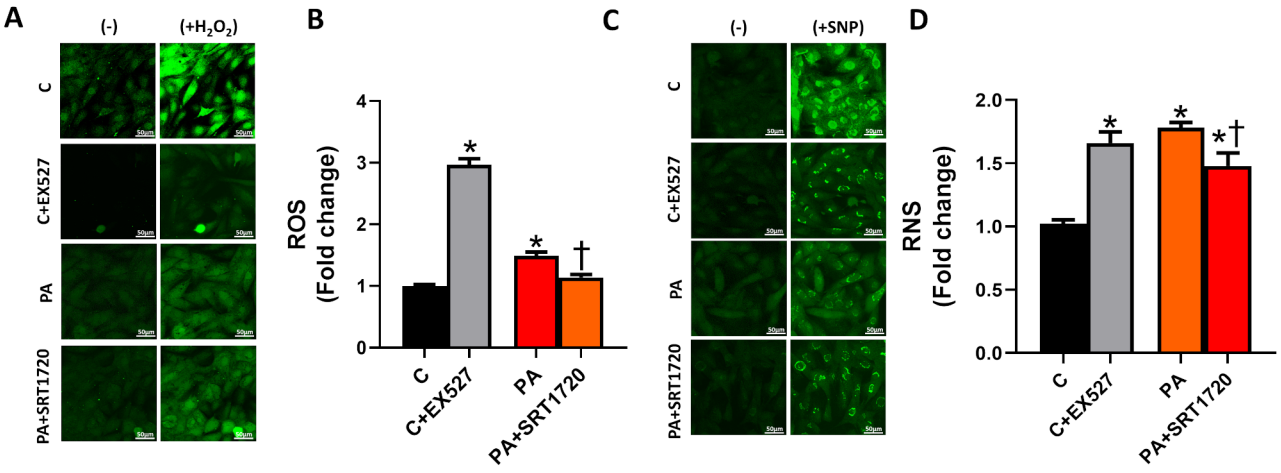

Fig. 3 The role of SIRT1 inhibition and palmitic acid (PA)-induced insulin resistance on the levels of reactive oxygen and nitrogen species (ROS and RNS). ROS and RNS are measured in control (**C**) cells incubated with and without SIRT1 inhibitor (EX527;10μM), PA-treated insulin-resistant cells incubated with and without SIRT1 activator (SRT1720;2μM) for 24 h. (**A**) The confocal images representative of ROS measurements and (**B**) their mean values depicted as a bar graph (fold change). (**C**) The confocal images representative of RNS measurements and (**D**) their mean values depicted as a bar graph (fold change). EX527 was used as an inhibitor, and SRT1720 as an activator of SIRT1 Bars are represented as mean (± SEM). The total number of cells used per group; n_{cells}=15–25. Significance level accepted at $^{*}p < 0.05$ vs. C, and $^{\dagger}p < 0.05$ vs. PA

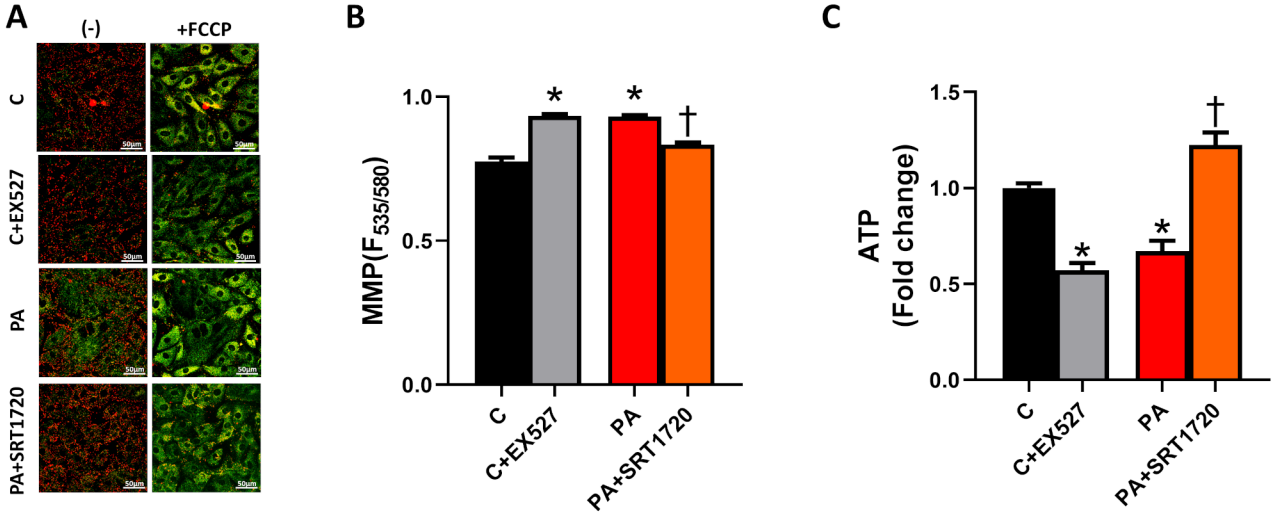

Fig. 4 The role of SIRT1 inhibition and palmitic acid (PA)-induced insulin resistance on the levels of mitochondrial membrane potential (MMP) and ATP production. MMP and ATP level are measured in control (**C**) cells incubated with and without SIRT1 inhibitor (EX527;10μM), PA-treated insulin-resistant cells incubated with and without SIRT1 activator (SRT1720;2μM) for 24 h. The representative ratio-metric original confocal traces (**A**) to determine the level of the mitochondrial membrane potential (MMP) in cells loaded with cell permeable JC-1 dye (5μM, 30 min) and (**B**) their mean values as bar graph. The dye was excited at 488 nm, and the emission was collected at both 535 nm (green signal; cytosolic accumulation of the dye) and 585 nm (red signal; mitochondrial accumulation of the dye). The mitochondria were depolarized, to calibrate the changes in MMP, with Carbonyl cyanide 4-trifluoromethoxy phenylhydrazone (FCCP; 5 μM). (**C**) Total ATP production was measured using a Luminescent based cell viability assay kit (Promega, G9241). EX527 was used as an inhibitor, and SRT1720 as an activator of SIRT1. The mean values represented as bar graph. Bars represent as mean (± SEM). The total number of cells used per group; n_{cell}=90–70. Significance level accepted at $^{*}p < 0.05$ vs. C, and $^{\dagger}p < 0.05$ vs. PA

K-acetylation in control cells and SIRT1 activation in insulin-resistant H9c2 cells on ATP production. As illustrated in Fig. 4C, SIRT1 inhibition resulted in decreased ATP production, whereas SIRT1 activation in insulin-resistant H9c2 cells led to a significant increase.

The balance between mitochondrial fusion and fission in the heart plays a crucial role in maintaining mitochondrial quality control, energy production, cellular signaling, and cellular responses to stressors, all of which collectively impact cardiac function and overall health [37, 49]. Here, we measured mitochondrial fusion and fission markers including Mfn1, Mfn2, and Fis1. We observed that the mitochondrial fusion marker Mfn2 is reduced PA induced insulin-resistant H9c2 cells, without

altering the Mfn1 protein level significantly (Fig. 5A-C). The Mfn1/Mfn2 ratio typically indicates a preference for mitochondrial fusion, correlating with heightened mitochondrial connectivity, elongated mitochondria, and improved mitochondrial function. Our findings revealed that the Mfn1/Mfn2 ratio was elevated in SIRT1 inhibition in control and insulin-resistant cells, while SIRT1 activation effectively restored the Mfn1/Mfn2 ratio to control levels (Fig. 5D). Conversely, the Fis1 protein level remained unchanged, regardless of SIRT1 inhibition by EX527 in control cells or SIRT1 activation by SRT1720 in insulin-resistant cells (Fig. 5E and F).

The Bax/Bcl-2 ratio within a cell determines its apoptosis status, representing the proportion of pro-apoptotic Bax protein to anti-apoptotic Bcl-2 protein. We observed an increase in the Bax/Bcl-2 ratio in both control cells with SIRT1 activation and insulin-resistant cells. Nevertheless, SIRT1 activation in insulin-resistant cells provided protection against apoptosis (Fig. 5G and H).

Discussion

In the current study, we demonstrated that activating SIRT1 in insulin-resistant hearts improves mitochondrial function via altering intracellular ion balance and preventing apoptosis.

Current results prove that levels of K-acetylation markedly increased insulin-resistant H9c2 cells. Furthermore, SRT1720 treatment in PA-induced insulin resistance for SIRT1 activation led to a complete restoration of the K-acetylation level. Conversely, inhibiting SIRT1 in control cells using EX527 resulted in an increased total K-acetylation in H9c2 cells. These findings highlight the critical role of SIRT1 in modulating protein K-acetylation both in control and PA-treated cells. It has been well documented that hyper K-acetylation causes drastic alterations in cellular stress response, depressed mitochondrial function, and impaired contractility in cardiomyocytes [31, 50–52]. Romanic et al. showed that K-acetylation of the titin proteins was increased in obese mice, which caused increased myocardial stiffness, impaired diastolic function, and decreased contractility [53]. Additionally, in failing hearts, SERCA, a crucial contractile protein responsible for regulating intracellular Ca^{2+} levels, undergo K-acetylation, resulting in reduced SERCA2a activity [54]. However, deacetylation of SERCA2a through SIRT1 activation preserves its function and mitigates cardiac defects in failing hearts [54]. Dysregulated $[Ca^{2+}]_i$ homeostasis in cardiomyocytes can lead to several detrimental effects including, cardiac arrhythmias, contractile dysfunction, mitochondrial dysfunction, cellular stress, and apoptosis [55–57]. According to current data,

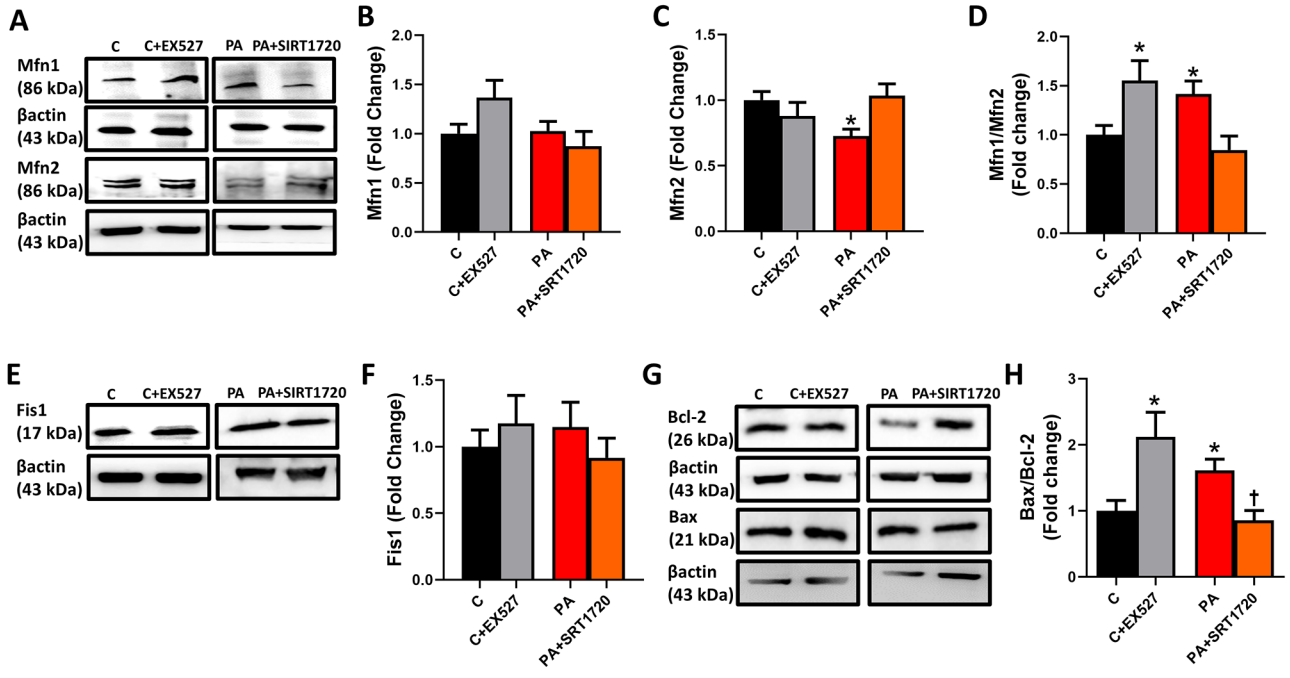

Fig. 5 The role of SIRT1 inhibition and palmitic acid (PA)-induced insulin resistance on mitochondrial dynamics and apoptosis. (**A**) Representative Western blot images of Mfn1 (measured at 86 kDa), Mfn2 (measured at 86 kDa), and β-Actin (measured at 43 kDa). (**B**) Mean values of Mfn1, (**C**) Mfn2, (**D**) Mfn1/Mfn2 ratio are given as bar graph. (**E**) Representative Western blot images of Fis1, and β-Actin measured at 86 kDa and 43 kDa, respectively. (**F**) Mean value of Fis1 protein level is given as bar graph (**G**) The relative densitometric changes in the protein ratio of Bax (measured at 21 kDa) to Bcl-2 (measured at 26 kDa) and (**H**) mean values in the groups of cells are given as bar graph. EX527 was used as an inhibitor, and SRT1720 as an activator of SIRT1. Bars represent as mean (± SEM). $N = 5–10$. Significance level accepted at $^{*}p < 0.05$ vs. C, and $^{\dagger}p < 0.05$ vs. PA

$[Ca^{2+}]_i$ levels significantly increased in insulin-resistant and SIRT1 inhibited cells. $[Ca^{2+}]_i$ level increase in insulin-resistant cells was normalized by SIRT1720-induced SIRT1 activation. The result that we observed at the cellular level is consistent with the diabetic cardiomyopathy pathophysiology and also explains the link between SIRT1 activation and cardiac functional recovery.

In current study, we analyzed Fis1, MFN1 and MFN2 levels to understand the mitochondrial fusion and fission dynamics. MFN1 and Fis1 did not differ among groups whereas MFN2 levels were markedly decreased in insulin-resistant animals. Moreover, SIRT1 activation (SRT1720) in these animals was normalized MFN2 levels. In the literature, MFN2 expression has been found to be reduced in obese and type II diabetic animals [58, 59]. Zorzano et al. assessed the levels of MFN2 in muscle samples taken from diabetic patients and observed a decrease in MFN2 levels, which is correlated with impaired mitochondrial function in skeletal muscle [60]. Furthermore, amelioration of insulin sensitivity by bariatric surgery is associated with an increased Mfn2 expression in skeletal muscle [60]. Gao et al. conducted a longitudinal study and evaluated the alteration of MFN2 levels by duration of STZ-induced diabetes. According to their results MFN2 expression is gradually lowered in cardiac tissue starting from 4th week reaching to 12th week and it is accompanied by a gradual increase in oxidative stress and apoptosis [61]. Since MFNs regulates tethering of the mitochondria, reduction of MFN2 in insulin-resistant animals may increase mitochondrial fragmentation. Besides, MFN1-knock out animals (KO) exhibit short mitochondrial tubules or tiny mitochondrial spheres with uniform size, and MFN2-KO cells show swollen spherical or short-rod mitochondria with a diameter several times larger than wild type mitochondrion [62]. These morphological alterations further impair the mitochondrial function alongside with the fragmentation. In our earlier research, we also demonstrated that H9c2 cells treated with palmitic acid (PA) exhibited mitochondrial swelling and loss of cristae, along with autolysosomes containing residual bodies [41]. Changes in mitochondrial dynamics can impact mitochondrial function within cells. In order to comprehend the influence of these dynamic changes, we evaluated ATP production and mitochondrial membrane potential (MMP), both of which serve as direct indicators of mitochondrial function.

ATP production is markedly reduced in PA and SIRT1 inhibition (EX527) groups and restored by SIRT1 activation (SRT1720) in PA cells. Parallelly, MMPs became more depolarized in PA and SIRT1 inhibition groups and normalized by SIRT1 activation. Current results are consistent with the literature. Hou et al. measured the MMP and ATP production to evaluate mitochondrial function in STZ-induced diabetic nephropathy model and demonstrated a mitochondrial depolarization and impaired ATP production [63]. Recently, Veeranki et al. used a db/db mice model to induce obesity in mice and observed an enhanced mitochondrial fission, a depolarization trend in MMPs and a reduction in ATP production in cardiac tissue [64].

As $[Ca^{2+}]_i$ homeostasis in the cells, $[Zn^{2+}]_i$ has also an important role of the regulation of the cellular function. Accumulating evidence suggests that K-acetylation serves as a crucial regulatory mechanism influencing the activity of zinc-binding proteins and zinc-dependent enzymes, thereby impacting various cellular processes such as DNA repair, apoptosis, and oxidative stress response [65].

It is well known that, increases in $[Zn^{2+}]_i$ in the cell can activate histone deacetylase activity, results in a more compact and condensed chromatin structure, leading to reduced gene expression involved in cell cycle regulation, differentiation [66, 67]. In our previous studies, we have also showed that changes of the mitochondrial zinc transporter ZnT6 and ZnT7 expression level in cardiomyocytes effects the epigenetic regulation in cardiomyocytes through histone modification, via changes the mitochondrial and cytosolic $[Zn^{2+}]$ [65, 68]. In current study, we observed that inhibition of the SIRT1 with EX5720 or in insulin-resistant cardiomyocytes exhibited high $[Ca^{2+}]_i$ and $[Zn^{2+}]_i$ and this increase is prevented by SIRT1 activation in insulin-resistant H9c2 cells, which may affect the mitochondrial dynamics. We demonstrated that an increase in total or mitochondrial $[Zn^{2+}]$ resulted in the depolarization of MMP and impaired mitochondrial dynamics together with the elevated ROS production [65, 68].

ROS and RNS have important physiological roles in cardiomyocyte function, their excessive production or dysregulation can contribute to oxidative stress, inflammation, and cell death, all of which are implicated in the pathogenesis of cardiovascular diseases [69, 70]. We have also found that ROS and RNS production was significantly elevated in PA induced insulin-resistant cells and through SIRT1 inhibition. Activation of the SIRT1 in PA cells completely or partially restored the ROS and RNS, respectively. Oxidative stress is linked to the pathogenesis of various diseases, including cardiovascular diseases, neurodegenerative disorders, and cancer [71]. Boosting antioxidant defences through increased expression of antioxidant proteins can help mitigate disease development or progression. In our previous studies we demonstrated that Type1 diabetic and metabolic syndrome rats showed increased in ROS and RNS production [38, 41, 72]. Elevated levels of ROS and RNS lead to an increase in $[Ca^{2+}]_i$ and $[Zn^{2+}]_i$ in cardiomyocytes [47, 48]. On the other hand, it causes phosphorylation of contractile proteins, an increase in calcium sparks, a decrease in Ca^{2+}

transients and in endoplasmic reticulum (ER) [Ca^{2+}], inhibition of voltage-gated L-type calcium channels, and ultimately contributes to contractile dysfunction [39, 47, 48]. However, treating cells with antioxidants or antioxidant-like compounds inhibited the production of ROS and RNS induced by hyperglycemia and restored cardiac function [39, 73]. It has been also showed that SIRT1 activation with SRT1720 decreased the RNS in oxidative stress-induced mice embryos [74]. These findings suggest that activating SIRT1 may enhance antioxidant capacity and prevent cellular damage. Conversely, inhibiting SIRT1 reduces antioxidant capacity and leads to cellular damage potentially, associated with increased production of ROS and RNS.

Current results showed that SIRT1 inhibition and treatment with PA led to increased apoptosis (increased Bax/Bcl-2 ratio). Activating SIRT1 in cells treated with PA restored antioxidant capacity. Increased production of ROS and RNS, along with disrupted mitochondrial dynamics, can contribute to increased apoptosis. Furthermore, the beneficial effects of SIRT1 on cellular function are potentially linked to restored ROS production, improved $[Ca^{2+}]_i$ and [Zn^{2+}], and enhanced mitochondrial function, leading to reduced apoptosis.

In the current study, we preferred palmitate incubation to induce insulin resistance in H9c2 cells. Palmitate incubation increases the synthesis of sphingolipids especially the *de novo* synthesis of ceramide which is a metabolic derivative of palmitate [75]. Increased level of ceramides triggers apoptosis in various cell types [76]. Thus, the increased apoptotic response that we have observed in PA-treated cells may be related to deranged ceramide signaling. Palmitate also causes a molecular process called protein palmitoylation which is simply attachment of palmitate moieties to cysteine residues [77]. Since protein palmitoylation may also affect protein function and stability, we have to consider the possible effects of this process on our findings.

Conclusion

Our findings underscore the detrimental effects of palmitic acid-induced insulin resistance, particularly in relation to K-acetylation-mediated alterations. This includes disruptions in intracellular ionic homeostasis, mitochondrial function, increased apoptosis, and subsequent cardiac dysfunction. However, the activation of SIRT1 serves as a protective mechanism, mitigating these adverse effects and preserving cellular and cardiac health. On the other hand, we need to be cautious before translating

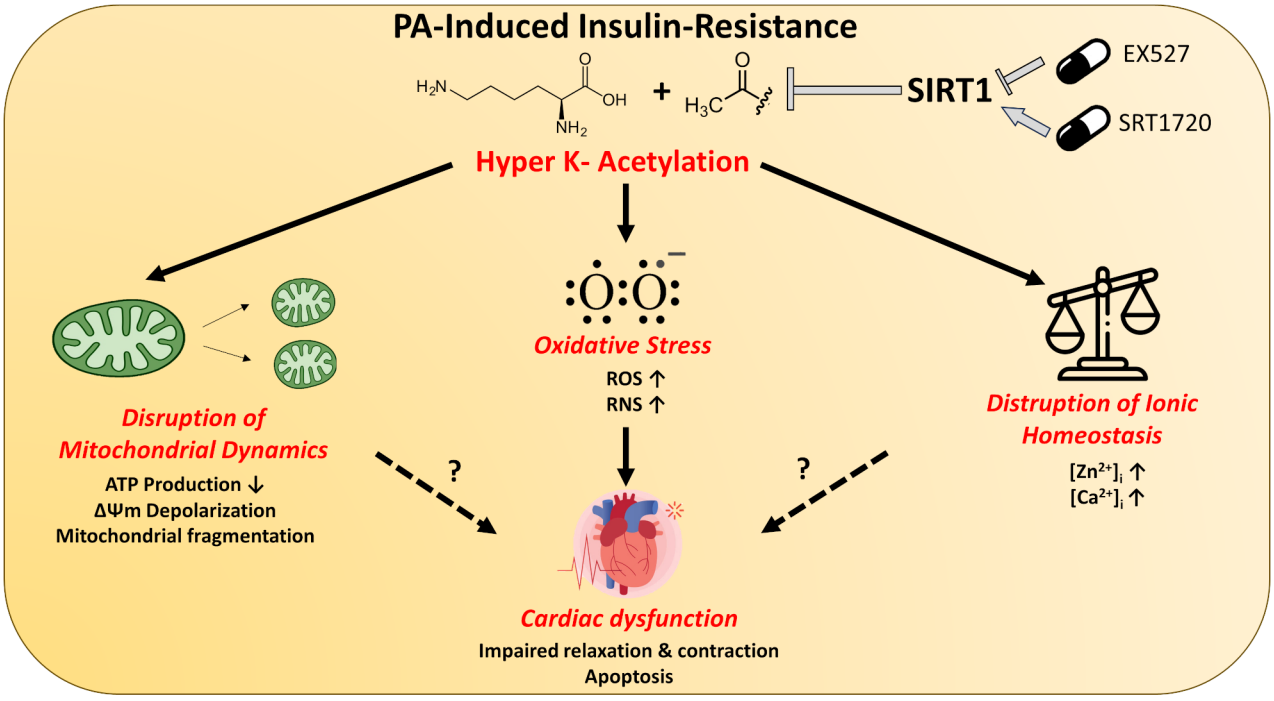

Fig. 6 Cellular alterations in palmitic acid (PA)-induced insulin resistance model in H9c2 cells. Insulin-resistance markedly increased the acetylation of lysine residues in peptide chains (Hyper K-Acetylation). Hyper K-Acetylation caused mitochondrial dysfunction which was reflected in mitochondrial fragmentation, lowered ATP production, and mitochondrial membrane (ΔΨm) depolarization. Parallelly K-acetylation increased cellular oxidative stress which affected the levels of ROS and RNS. Cellular ionic homeostasis was impaired. Intracellular free zinc ($[Zn^{2+}]_i$) and free calcium ($[Ca^{2+}]_i$) concentrations were increased. All these alterations caused increased apoptosis and impaired contractile function both of which are hallmarks of cardiac dysfunction. SIRT1 is one of the major regulators of intracellular K-acetylation levels. EX527 was used as an inhibitor, and SRT1720 as an activator of SIRT1

H9c2 data to the insulin-resistant heart. Although cellular insulin resistance models give us plenty of opportunities to reveal the effects of various therapeutic strategies, they still cannot model every aspect of the organism in a petri dish. Yet still, the therapeutic value of SIRT1 activation in insulin resistance-related cardiac complications bears a potential and needs to be studied in future studies. (Fig. 6).

Abbreviations

PTMs	Post-translational modifications
K-acetylation	Lysine-acetylation
SIRTs	Sirtuins
SERCA2a	Cardiac sarcoplasmic reticulum calcium ATPase
NAD^+	Nicotinamide adenine dinucleotide
MFNs	Mitofusins
FIS1	Fission 1 protein
$[Zn^{2+}]_i$	Intracellular free zinc levels
PVDF	Polyvinylidene difluoride
ΔΨM	Mitochondrial membrane potential
ROS	Reactive oxygen species
RNS	Reactive nitrogen species
DCFDA	Chloromethyl-2′,7′-dichlorodihydrofuorescein diacetate
DAF	Diacetate 4-Amino-5-Methylamino-2′,7′-Difluorofluorescein Diacetate
NO	Nitric oxide
SNP	Sodium nitroprusside
H_2O_2	Hydrogen peroxide
ZnPT	Zn^{2+}-pyrithione
TPEN	N, N, N′, N′-tetrakis (2-pyridylmethyl) ethylenediamine
$[Ca^{2+}]_i$	Intracellular Free Calcium
PA	Palmitic acid
ER	Endoplasmic reticulum

Supplementary Information

The online version contains supplementary material available at https://doi.org/10.1186/s12872-024-04397-7.

Supplementary Material 1

Supplementary Material 2

Acknowledgements

We would like to express our sincere gratitude to our undergraduate students Semanur Isik, Mehmet Utku Sevinc, Enes Bugrahan Sarikaya, and Ece Tuana Erdogan for their invaluable contributions to this research.

Author contributions

E.T.: Coordinated the study, Improved the methodology, performed the experiments, contributed to analyzing the data, writing- original draft preparation, writing, reviewing, and editing. B.S.: Performed the experiments and analyzed the data. G.A.: Performed the experiments and analyzed the data. D.I: Performed the experiments and analyzed the data. F.T.S.: Performed the experiments and analyzed the data. L.A.: Performed the experiments and analyzed the data. S.Ş.: Performed the experiments and analyzed the data. F.A. Review, and edit the manuscript.

Funding

This study was supported by the Scientific and Technological Research Council of Turkiye (No. SBAG-222S502) and 2209-A Research Project Support Programme for Undergraduate Students (1919B012100837).

Data availability

The datasets used and/or analysed during the current study are available from the corresponding author on reasonable request.

Declarations

Ethics approval and consent to participate

Not applicable.

Consent for publication

Not applicable.

Competing interests

The authors declare no competing interests.

Received: 6 May 2024 / Accepted: 4 December 2024
Published online: 29 March 2025

References

1. Lebovitz HE. Insulin resistance: definition and consequences. Exp Clin Endocrinol Diabetes. 2001;109(Suppl 2):S135–148.
2. Huang PL. A comprehensive definition for metabolic syndrome. Dis Model Mech. 2009;2(5–6):231–7.
3. Yudhani RD, Sari Y, Nugrahaningsih DAA, Sholikhah EN, Rochmanti M, Purba AKR, Khotimah H, Nugrahenny D, Mustofa M. In Vitro Insulin Resistance Model: A Recent Update. *J Obes* 2023, 2023:1964732.
4. Wang YC, Peterson SE, Loring JF. Protein post-translational modifications and regulation of pluripotency in human stem cells. Cell Res. 2014;24(2):143–60.
5. Schaffert LN, Carter WG. Do post-translational modifications influence protein aggregation in neurodegenerative diseases: a systematic review. Brain Sci 2020, 10(4).
6. Xu H, Wang Y, Lin S, Deng W, Peng D, Cui Q, Xue Y. PTMD: a database of Human Disease-associated post-translational modifications. Genomics Proteom Bioinf. 2018;16(4):244–51.
7. Pietrafesa G, De Zio R, Scorza SI, Armentano MF, Pepe M, Forleo C, Procino G, Gerbino A, Svelto M, Carmosino M. Targeting unfolded protein response reverts ER stress and ER ca(2+) homeostasis in cardiomyocytes expressing the pathogenic variant of Lamin A/C R321X. J Transl Med. 2023;21(1):340.
8. Tuncay E, Gando I, Huo JY, Yepuri G, Sampler N, Turan B, Yang HQ, Ramasamy R, Coetzee WA. The cardioprotective role of sirtuins is mediated in part by regulating K(ATP) channel surface expression. Am J Physiol Cell Physiol. 2023;324(5):C1017–27.
9. Theillet FX, Smet-Nocca C, Liokatis S, Thongwichian R, Kosten J, Yoon MK, Kriwacki RW, Landrieu I, Lippens G, Selenko P. Cell signaling, post-translational protein modifications and NMR spectroscopy. J Biomol NMR. 2012;54(3):217–36.
10. Müller MM. Post-translational modifications of protein backbones: unique functions, mechanisms, and challenges. Biochemistry. 2018;57(2):177–85.
11. Kislenko E, İncel A, Gawlitza K, Sellergren B, Rurack K. Towards molecularly imprinted polymers that respond to and capture phosphorylated tyrosine epitopes using fluorescent bis-urea and bis-imidazolium receptors. J Mater Chem B. 2023;11(45):10873–82.
12. Zhao P, Malik S. The phosphorylation to acetylation/methylation cascade in transcriptional regulation: how kinases regulate transcriptional activities of DNA/histone-modifying enzymes. Cell Biosci. 2022;12(1):83.
13. Francois A, Canella A, Marcho LM, Stratton MS. Protein acetylation in cardiac aging. J Mol Cell Cardiol. 2021;157:90–7.
14. Dubois-Deruy E, El Masri Y, Turkieh A, Amouyel P, Pinet F, Annicotte JS. Cardiac Acetylation in Metabolic diseases. Biomedicines 2022, 10(8).
15. Yang M, Zhang Y, Ren J. Acetylation in cardiovascular diseases: molecular mechanisms and clinical implications. Biochim et Biophys Acta (BBA) - Mol Basis Disease. 2020;1866(10):165836.
16. Tanno M, Kuno A, Horio Y, Miura T. Emerging beneficial roles of sirtuins in heart failure. Basic Res Cardiol. 2012;107:1–14.
17. Ianni A, Yuan X, Bober E, Braun T. Sirtuins in the cardiovascular system: potential targets in pediatric cardiology. Pediatr Cardiol. 2018;39:983–92.
18. Dong Q, Wu Z, Li X, Yan J, Zhao L, Yang C, Lu J, Deng J, Chen M. Resveratrol ameliorates cardiac dysfunction induced by pressure overload in rats via structural protection and modulation of ca(2+) cycling proteins. J Transl Med. 2014;12:323.
19. Sulaiman M, Matta MJ, Sunderesan NR, Gupta MP, Periasamy M, Gupta M. Resveratrol, an activator of SIRT1, upregulates sarcoplasmic calcium ATPase and improves cardiac function in diabetic cardiomyopathy. Am J Physiol Heart Circ Physiol. 2010;298(3):H833–843.

20. Cao Y, Jiang X, Ma H, Wang Y, Xue P, Liu Y. SIRT1 and insulin resistance. J Diabetes Complicat. 2016;30(1):178–83.
21. Liang F, Kume S, Koya D. SIRT1 and insulin resistance. Nat Reviews Endocrinol. 2009;5(7):367–73.
22. Filadi R, Pendin D, Pizzo P. Mitofusin 2: from functions to disease. Cell Death Dis. 2018;9(3):330.
23. Wai T, Langer T. Mitochondrial dynamics and metabolic regulation. Trends Endocrinol Metab. 2016;27(2):105–17.
24. Pendin D, Filadi R, Pizzo P. The Concerted Action of Mitochondrial Dynamics and Positioning: new characters in Cancer Onset and Progression. Front Oncol. 2017;7:102.
25. Gomes LC, Di Benedetto G, Scorrano L. During autophagy mitochondria elongate, are spared from degradation and sustain cell viability. Nat Cell Biol. 2011;13(5):589–98.
26. James DI, Parone PA, Mattenberger Y, Martinou JC. hFis1, a novel component of the mammalian mitochondrial fission machinery. J Biol Chem. 2003;278(38):36373–9.
27. Santel A, Fuller MT. Control of mitochondrial morphology by a human mitofusin. J Cell Sci. 2001;114(Pt 5):867–74.
28. Brito S, Lee MG, Bin BH, Lee JS. Zinc and its transporters in Epigenetics. Mol Cells. 2020;43(4):323–30.
29. López JE, Sullivan ED, Fierke CA. Metal-dependent deacetylases: Cancer and epigenetic regulators. ACS Chem Biol. 2016;11(3):706–16.
30. Xia C, Tao Y, Li M, Che T, Qu J. Protein acetylation and deacetylation: an important regulatory modification in gene transcription (review). Exp Ther Med. 2020;20(4):2923–40.
31. Anderson KA, Hirschey MD. Mitochondrial protein acetylation regulates metabolism. Essays Biochem. 2012;52:23–35.
32. Waddell J, Banerjee A, Kristian T. Acetylation in Mitochondria Dynamics and Neurodegeneration. Cells 2021, 10(11).
33. Hu Q, Zhang H, Gutiérrez Cortés N, Wu D, Wang P, Zhang J, Mattison JA, Smith E, Bettcher LF, Wang M, et al. Increased Drp1 acetylation by lipid overload induces Cardiomyocyte Death and Heart Dysfunction. Circul Res. 2020;126(4):456–70.
34. Thiagarajan D, Vedantham S, Ananthakrishnan R, Schmidt AM, Ramasamy R. Mechanisms of transcription factor acetylation and consequences in hearts. Biochim Biophys Acta. 2016;1862(12):2221–31.
35. Okatan EN, Olgar Y, Tuncay E, Turan B. Azoramide improves mitochondrial dysfunction in palmitate-induced insulin resistant H9c2 cells. Mol Cell Biochem. 2019;461(1–2):65–72.
36. Billur D, Tuncay E, Okatan EN, Olgar Y, Durak AT, Degirmenci S, Can B, Turan B. Interplay between cytosolic free zn 2 + and mitochondrion morphological changes in rat ventricular cardiomyocytes. Biol Trace Elem Res. 2016;174:177–88.
37. Tuncay E, Bitirim CV, Olgar Y, Durak A, Rutter GA, Turan B. Zn(2+)-transporters ZIP7 and ZnT7 play important role in progression of cardiac dysfunction via affecting sarco(endo)plasmic reticulum-mitochondria coupling in hyperglycemic cardiomyocytes. Mitochondrion. 2019;44:41–52.
38. Tuncay E, Olgar Y, Durak A, Degirmenci S, Bitirim CV, Turan B. β(3) -adrenergic receptor activation plays an important role in the depressed myocardial contractility via both elevated levels of cellular free zn(2+) and reactive nitrogen species. J Cell Physiol. 2019;234(8):13370–86.
39. Tuncay E, Okatan EN, Vassort G, Turan B. ß-blocker timolol prevents arrhythmogenic Ca^{2+} release and normalizes Ca^{2+} and Zn^{2+} dyshomeostasis in hyperglycemic rat heart. PLoS ONE. 2013;8(7):e71014.
40. Goktas Sahoglu S, Kazci YE, Tuncay E, Torun T, Akdeniz C, Tuzcu V, Cagavi E. Functional evaluation of the tachycardia patient-derived iPSC cardiomyocytes carrying a novel pathogenic SCN5A variant. J Cell Physiol. 2022;237(10):3900–11.
41. Olgar Y, Tuncay E, Billur D, Durak A, Ozdemir S, Turan B. Ticagrelor reverses the mitochondrial dysfunction through preventing accumulated autophagosomes-dependent apoptosis and ER stress in insulin-resistant H9c2 myocytes. Mol Cell Biochem. 2020;469(1–2):97–107.
42. Yang J, Song C, Zhan X. The role of protein acetylation in carcinogenesis and targeted drug discovery. Front Endocrinol (Lausanne). 2022;13:972312.
43. Zhang Y, Zhou F, Bai M, Liu Y, Zhang L, Zhu Q, Bi Y, Ning G, Zhou L, Wang X. The pivotal role of protein acetylation in linking glucose and fatty acid metabolism to β-cell function. Cell Death Dis. 2019;10(2):66.
44. Kabir F, Atkinson R, Cook AL, Phipps AJ, King AE. The role of altered protein acetylation in neurodegenerative disease. Front Aging Neurosci. 2022;14:1025473.
45. Wątroba M, Szewczyk G, Szukiewicz D. The role of Sirtuin-1 (SIRT1) in the physiology and pathophysiology of the human placenta. Int J Mol Sci 2023, 24(22).
46. Olgar Y, Turan B. A sodium-glucose cotransporter 2 (SGLT2) inhibitor dapagliflozin comparison with insulin shows important effects on Zn2+-transporters in cardiomyocytes from insulin-resistant metabolic syndrome rats through inhibition of oxidative stress. Can J Physiol Pharmacol. 2019;97(6):528–35.
47. Tuncay E, Bilginoglu A, Sozmen NN, Zeydanli EN, Ugur M, Vassort G, Turan B. Intracellular free zinc during cardiac excitation-contraction cycle: calcium and redox dependencies. Cardiovasc Res. 2011;89(3):634–42.
48. Tuncay E, Turan B. Intracellular zn(2+) increase in Cardiomyocytes induces both Electrical and Mechanical Dysfunction in Heart via Endogenous Generation of reactive Nitrogen species. Biol Trace Elem Res. 2016;169(2):294–302.
49. Chen H, Detmer SA, Ewald AJ, Griffin EE, Fraser SE, Chan DC. Mitofusins Mfn1 and Mfn2 coordinately regulate mitochondrial fusion and are essential for embryonic development. J Cell Biol. 2003;160(2):189–200.
50. Dikalov SI, Dikalova AE. Crosstalk between mitochondrial hyperacetylation and oxidative stress in vascular dysfunction and hypertension. Antioxid Redox Signal. 2019;31(10):710–21.
51. Loescher CM, Hobbach AJ, Linke WA. Titin (TTN): from molecule to modifications, mechanics, and medical significance. Cardiovasc Res. 2022;118(14):2903–18.
52. Foster DB, Liu T, Rucker J, O'Meally RN, Devine LR, Cole RN. O'Rourke B: the cardiac acetyl-lysine proteome. PLoS ONE. 2013;8(7):e67513.
53. Romanick SS, Ulrich C, Schlauch K, Hostler A, Payne J, Woolsey R, Quilici D, Feng Y, Ferguson BS. Obesity-mediated regulation of cardiac protein acetylation: parallel analysis of total and acetylated proteins via TMT-tagged mass spectrometry. Biosci Rep 2018, 38(5).
54. Gorski PA, Jang SP, Jeong D, Lee A, Lee P, Oh JG, Chepurko V, Yang DK, Kwak TH, Eom SH, et al. Role of SIRT1 in modulating Acetylation of the Sarco-endoplasmic reticulum ca(2+)-ATPase in Heart failure. Circ Res. 2019;124(9):e63–80.
55. Eisner DA, Caldwell JL, Kistamás K, Trafford AW. Calcium and excitation-contraction coupling in the heart. Circ Res. 2017;121(2):181–95.
56. Sutanto H, Lyon A, Lumens J, Schotten U, Dobrev D, Heijman J. Cardiomyocyte calcium handling in health and disease: insights from in vitro and in silico studies. Prog Biophys Mol Biol. 2020;157:54–75.
57. Luo M, Anderson ME. Mechanisms of altered Ca^{2+} handling in heart failure. Circ Res. 2013;113(6):690–708.
58. Bach D, Naon D, Pich S, Soriano FX, Vega N, Rieusset J, Laville M, Guillet C, Boirie Y, Wallberg-Henriksson H, et al. Expression of Mfn2, the Charcot-Marie-tooth neuropathy type 2A gene, in human skeletal muscle: effects of type 2 diabetes, obesity, weight loss, and the regulatory role of tumor necrosis factor alpha and interleukin-6. Diabetes. 2005;54(9):2685–93.
59. Bach D, Pich S, Soriano FX, Vega N, Baumgartner B, Oriola J, Daugaard JR, Lloberas J, Camps M, Zierath JR, et al. Mitofusin-2 determines mitochondrial network architecture and mitochondrial metabolism. A novel regulatory mechanism altered in obesity. J Biol Chem. 2003;278(19):17190–7.
60. Zorzano A, Liesa M, Palacín M. Mitochondrial dynamics as a bridge between mitochondrial dysfunction and insulin resistance. Arch Physiol Biochem. 2009;115(1):1–12.
61. Gao Q, Wang XM, Ye HW, Yu Y, Kang PF, Wang HJ, Guan SD, Li ZH. Changes in the expression of cardiac mitofusin-2 in different stages of diabetes in rats. Mol Med Rep. 2012;6(4):811–4.
62. Chen L, Liu B, Qin Y, Li A, Gao M, Liu H, Gong G. Mitochondrial Fusion protein Mfn2 and its role in Heart failure. Front Mol Biosci. 2021;8:681237.
63. Hou Y, Li S, Wu M, Wei J, Ren Y, Du C, Wu H, Han C, Duan H, Shi Y. Mitochondria-targeted peptide SS-31 attenuates renal injury via an antioxidant effect in diabetic nephropathy. Am J Physiol Ren Physiol. 2016;310(6):F547–559.
64. Veeranki S, Givvimani S, Kundu S, Metreveli N, Pushpakumar S, Tyagi SC. Moderate intensity exercise prevents diabetic cardiomyopathy associated contractile dysfunction through restoration of mitochondrial function and connexin 43 levels in db/db mice. J Mol Cell Cardiol. 2016;92:163–73.
65. Tuncay E, Aktay I, Turan B. Overexpression of Slc30a7/ZnT7 increases the mitochondrial matrix levels of labile zn(2+) and modifies histone modification in hyperinsulinemic cardiomyoblasts. J Trace Elem Med Biol. 2023;78:127198.
66. Flores BM, Uppalapati CK, Pascual AS, Vong A, Baatz MA, Harrison AM, Leyva KJ, Hull EE. Biological effects of HDAC inhibitors vary with zinc binding group: Differential effects on Zinc Bioavailability, ROS Production, and R175H p53 mutant protein reactivation. Biomolecules 2023, 13(11).

67. Parbin S, Kar S, Shilpi A, Sengupta D, Deb M, Rath SK, Patra SK. Histone deacetylases: a saga of perturbed acetylation homeostasis in cancer. J Histochem Cytochem. 2014;62(1):11–33.
68. Aktay I, Billur D, Tuncay E, Turan B. An overexpression of SLC30A6 gene contributes to Cardiomyocyte Dysfunction via affecting Mitochondria and Inducing activations in K-Acetylation and Epigenetic proteins. Biochem Genet 2023.
69. Turan B, Tuncay E. The role of labile zn(2+) and zn(2+)-transporters in the pathophysiology of mitochondria dysfunction in cardiomyocytes. Mol Cell Biochem. 2021;476(2):971–89.
70. Bou-Teen D, Kaludercic N, Weissman D, Turan B, Maack C, Di Lisa F, Ruiz-Meana M. Mitochondrial ROS and mitochondria-targeted antioxidants in the aged heart. Free Radic Biol Med. 2021;167:109–24.
71. Forman HJ, Zhang H. Targeting oxidative stress in disease: promise and limitations of antioxidant therapy. Nat Rev Drug Discovery. 2021;20(9):689–709.
72. Okatan EN, Tuncay E, Turan B. Cardioprotective effect of selenium via modulation of cardiac ryanodine receptor calcium release channels in diabetic rat cardiomyocytes through thioredoxin system. J Nutr Biochem. 2013;24(12):2110–8.
73. Tuncay E, Okatan EN, Toy A, Turan B. Enhancement of cellular antioxidant-defence preserves diastolic dysfunction via regulation of both diastolic Zn2 + and Ca2 + and prevention of RyR2-leak in hyperglycemic cardiomyocytes. Oxid Med Cell Longev. 2014;2014:290381.
74. Aksu K, Golal E, Aslan MA, Ustunel I, Acar N. The investigation of the role of sirtuin-1 on embryo implantation in oxidative stress-induced mice. J Assist Reprod Genet. 2021;38(9):2349–61.
75. Bandet CL, Tan-Chen S, Bourron O, Le Stunff H, Hajduch E. Sphingolipid metabolism: New Insight into Ceramide-Induced lipotoxicity in muscle cells. Int J Mol Sci 2019, 20(3).
76. Haimovitz-Friedman A, Kolesnick RN, Fuks Z. Ceramide signaling in apoptosis. Br Med Bull. 1997;53(3):539–53.
77. Schianchi F, Glatz JFC, Navarro Gascon A, Nabben M, Neumann D, Luiken J. Putative role of protein palmitoylation in Cardiac lipid-Induced insulin resistance. Int J Mol Sci 2020, 21(24).

Publisher's note